Journal of Innovative Applied Mathematics and Computational Sciences

J. Innov. Appl. Math. Comput. Sci. **2**(3) (2022), 69–85. n2t.net/ark:/49935/jiamcs.v2i3.25

http://jiamcs.centre-univ-mila.dz/

Modified projective synchronization of fractional-order hyperchaotic memristor-based Chua's circuit

Nadjet Boudjerida [1], Mohammed Salah Abdelouahab [1, 2] and René Lozi [3]

[1]Departement of Mathematics, Mentouri Brothers University of Constantine 1, Constantine, 25000, Algeria

[2]Laboratory of Mathematics and their interactions, Abdelhafid Boussouf University Center, Mila, 43000, Algeria

[3]Université Côte d'Azur, CNRS, LJAD, Nice 06108 France

Received 5 February 2022, Accepted 15 December 2022, Published 31 December 2022

Abstract. This paper investigates the modified projective synchronization (MPS) between two hyperchaotic memristor-based Chua circuits modeled by two nonlinear integer-order and fractional-order systems. First, a hyperchaotic memristor-based Chua circuit is suggested, and its dynamics are explored using different tools, including stability theory, phase portraits, Lyapunov exponents, and bifurcation diagrams. Another interesting property of this circuit was the coexistence of attractors and the appearance of mixed-mode oscillations. It has been shown that one can achieve MPS with integer-order and incommensurate fractional order memristor-based Chua circuits. Finally, examples of numerical simulation are presented, showing that the theoretical results are in good agreement with the numerical ones.

Keywords: Memristor; hyperchaotic system; Chua's circuit; Caputo derivative; incommensurate fractional order Hyperchaotic System; modified projective synchronization.
2020 Mathematics Subject Classification: 37M05, 37M20, 37M22, 37M25, 93D05

1 Introduction

In 1971, the circuit theorist Leon Chua had published a study entitled "Memristor: the missing circuit element". This achievement has attracted a great research attention across a wide range of disciplines, such as programmable logic [14] and electronics [33] as well as neural networks [42]. Because memristors are non-linear components, their application to build chaotic or hyperchaotic systems has received significant attention in recent decades [9,23,30]. For example, the canonical Chua's circuit has been improved by replacing its diode with a

✉Corresponding author. Email: boudjnadj1843@gmail.com

ISSN (electronic): 2773-4196

memristor whose output is monotone-increasing [8]. Both chaotic and hyperchaotic systems are clearly defined as nonlinear systems that are highly dependent on initial conditions, unpredictable in the long run and non-periodic. The fact that hyper-chaotic systems have at least two positive Lyapunov exponents makes their dynamics more complex. And hence favourable for many applications. Mainly, for encryption and secure communications [12,17,35,36]. Various models of commensurate fractional-order memristor-based systems have been designed [11,13,21]. However, because of the different fractional-order characteristics of each circuit component, it is more important to consider fractional-order circuits or systems with incommensurate fractional order. Meanwhile, synchronization of chaotic and hyperchaotic systems has become a crucial research domain, especially in secure communication [19]. Various techniques have been proposed for the synchronization of chaotic systems, such as Active control [31], adaptive control [4, 35], Feedback control, Prediction based feedback control, Sliding mode control and adaptive fuzzy control [2,5,6,10,31,34,38]. Using these methods, many works for the synchronization problem have been extended to the scope, such as phase synchronization, complete synchronization, anti-synchronization, projective synchronization, generalized projective synchronization, inverse hybrid function projective synchronization, generalized synchronization and MPS [4, 18, 29, 31, 41, 43], but there are few studies on the MPS between integer-order and incommensurate fractional order hyperchaotic systems.

Motivated by the precedent reasons, a hyperchaotic memristor-based Chua's circuit is suggested, and its dynamics are explored using different tools, including stability theory, phase portraits, Lyapunov exponents, and bifurcation diagrams. Then, using an active control strategy, the problem of MPS between integer-order and incommensurate fractional order hyperchaotic memristor-based systems is explored, and synchronization is proved using the Lyapunov stability theory of fractional systems.

The present paper is organized as follows: in section 2, a mathematical model of the memristor is described, and the Caputo fractional derivative is discussed. In section 3, a novel memristor-based hyperchaotic system is introduced and its dynamical behavior is investigated. MPS between integer-order and incommensurate fractional order hyperchaotic systems is applied using the active control method in section 4. To illustrate the theoretical results, numerical simulations are presented using MATLAB programs. Finally, in the last section, this study concludes with a summary of the accomplished results and a conclusion.

2 Preliminaries

2.1 Basic memristor model

A memristor is a nonlinear resistor with a memory effect that can be either flux-controlled or charge-controlled [8]. It can be defined as a dual-terminal device having the relationship

$$f(\varphi, q) = 0.$$

Equations (2.1) and (2.2) describe a charge-controlled and a flux-controlled memristor, respectively [20,26]

$$M(q) = \frac{d\varphi(q)}{dq}, v = M(q)i, \tag{2.1}$$

$$W(\varphi) = \frac{dq(\varphi)}{d\varphi}, i = W(\varphi)v, \tag{2.2}$$

Where φ denotes the magnetic flux and q the charge, $W(\varphi)$ and $M(q)$ are called the memductance and memristance respectively.
This study considers a flux-controlled memristor whose characteristics are described by a piecewise quadratic function $q(\varphi)$ given by

$$q(\varphi) = -a\varphi + 0.5b\varphi|\varphi|.$$

With a and b being positive parameters.
Hence, its memductance function is

$$W(\varphi) = \frac{dq(\varphi)}{d\varphi} = -a + b|\varphi|.$$

2.2 Caputo fractional derivative

Definition 2.1. The Caputo fractional derivative of order α of a continuous function $f : \mathbb{R}^+ \mapsto \mathbb{R}$ is defined by:

$$D_t^\alpha f(t) = \begin{cases} \frac{1}{\Gamma(m-\alpha)} \int_0^t \frac{f^{(m)}(\tau)}{(t-\tau)^{\alpha-m+1}} d\tau, & m-1 < \alpha < m, \\ \frac{d^m}{dt^m} f(t), & \alpha = m, \end{cases}$$

where $m = \lceil \alpha \rceil$, and Γ is the Γ-function defined by

$$\Gamma(z) = \int_0^{+\infty} e^{-t} t^{z-1} dt, \quad \Gamma(z+1) = z\Gamma(z).$$

Theorem 2.2. *Consider the incommensurate fractional order system*

$$D^{\alpha_i} x_i = f(x_1, x_2, ..., x_n, t), i = 1, 2, ..., n, \tag{2.3}$$

Where $\alpha_1 \neq \alpha_2 \neq ... \neq \alpha_n$. Suppose that m is the least common multiple of the denominators u_i's of α_i's, where $\alpha_i = \frac{v_i}{u_i}$, $u_i, v_i \in \mathbb{Z}^+$ for $i = 1, 2, ..., n$. Denote $\gamma = \frac{1}{m}$ and J be the Jacobian matrix $J = \frac{df}{dx}$ evaluated at the equilibrium, where $f = [f_1, f_2, ..., f_n]^T$, $x = [x_1, x_2, ..., x_n]^T$. System (2.3) is asymptotically stable if $|arg(\lambda_i)| > \gamma\frac{\pi}{2}$ is satisfied for all roots λ_i of the following equation :

$$det(diag([\lambda^{m\alpha_1}, \lambda^{m\alpha_2}, ..., \lambda^{m\alpha_n}]) - J) = 0, \tag{2.4}$$

3 Building a memristor-based system and its analysis

In this section, an alternative memristor-based Chua's circuit is proposed by replacing the nonlinear diode in the original circuit with a negative conductance and a passive flux-controlled memristor described by (2.2) in parallel and changing the inductance's position that becomes between the two capacitances as shown in Figure 2.1.
Kirchhoff Laws allow us to describe the suggested circuit theoretically by the following four-dimensional differential system

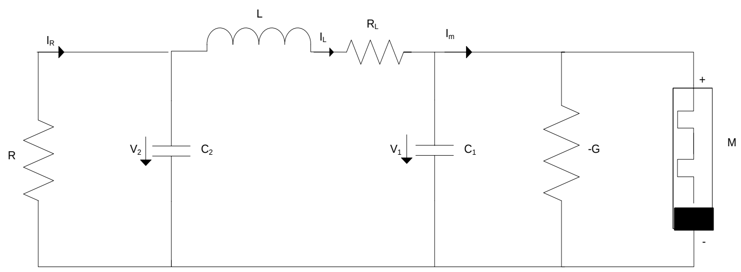

Figure 2.1: Modified memristor-based Chua's circuit

$$\begin{cases} \dfrac{dV_1(t)}{dt} = \dfrac{1}{C_1}\left[I_L(t) + GV_1(t) - W(\phi)\,V_1(t)\right], \\ \dfrac{dV_2(t)}{dt} = \dfrac{1}{C_2}\left[\dfrac{V_2(t)}{R} - I_L(t)\right], \\ \dfrac{dI_L(t)}{dt} = \dfrac{1}{L}\left[-V_1(t) + V_2(t) - R_L I_L(t)\right], \\ \dfrac{d\phi(t)}{dt} = V_1(t), \end{cases} \tag{3.1}$$

where $W(\phi)$ is defined by (2.2) and $V_i, i = 1.2$ voltages, R, R_L and G resistances, $C_i, i = 1.2$ capacitances, I_L current, L the inductance and ϕ the magnetic flux through the memristor. By setting $x = V_1,\ y = V_2,\ z = I_L,\ \omega = \phi,\ C_2 = 1, R = 1,\ \alpha = \dfrac{1}{C_1},\ \beta = \dfrac{1}{L},\ \gamma = \dfrac{R_L}{L}$ and $\xi = G$ then (3.1) can be converted into its dimensionless form

$$\begin{cases} \dot{x} = \alpha[z + \xi x - (-a + b|\omega|)x], \\ \dot{y} = y - z, \\ \dot{z} = -\beta(x - y) - \gamma z, \\ \dot{w} = x, \end{cases} \tag{3.2}$$

where x, y, z and ω are the states and α, β, γ, ξ, a and b are assumed to be positive constant parameters.

3.1 Stability analysis

The equilibrium points of system (3.2) are its solutions, taking each equation of the system equal to zero. Thus, the following equilibrium points are obtained

$$P_e = \{(x, y, z, \omega);\ x = 0,\ y = 0,\ z = 0 \text{ and } \omega = \omega_e \in \mathbb{R}\}. \tag{3.3}$$

Hence, each point on the $\omega -$ axis is an equilibrium point of (3.2), and (3.3) is called the equilibrium set.

The Jacobian matrix at each equilibrium point P_e is

$$J(P_e) = \begin{bmatrix} \alpha(\xi - W(w_e)) & 0 & \alpha & 0 \\ 0 & 1 & -1 & 0 \\ -\beta & \beta & -\gamma & 0 \\ 1 & 0 & 0 & 0 \end{bmatrix} \tag{3.4}$$

The characteristic polynomial of the system (3.2) is given by

$$\begin{aligned} P(\lambda) &= \lambda\left[\lambda^3 + [\gamma - 1 - \alpha(\xi - W(w_e))]\lambda^2 + [(-\gamma+1)\alpha(\xi - W(w_e)) + (1+\alpha)\beta - \gamma]\lambda \right. \\ &\quad \left. + \alpha[(\gamma-\beta)(\xi - W(w_e)) - \beta]\right] = \lambda Q(\lambda). \end{aligned} \tag{3.5}$$

Setting the system parameters as

$$\alpha = 5,\ \beta = 5,\ \gamma = 0.11,\ \xi = 3,\ a = 1.5,\ b = 1\ \ and\ \ W(\omega_e) = -a + b|\omega_e|. \tag{3.6}$$

Then, the characteristic polynomial (3.5) becomes

$$\begin{aligned} P(\lambda) &= \lambda Q(\lambda) \\ &= \lambda\left[\lambda^3 + (5\,|w_e| - 23.4)\,\lambda^2 + (50.15 - 4.5\,|w_e|)\,\lambda + 24.5\,|w_e| - 135.25\right] = 0. \end{aligned} \tag{3.7}$$

In order to find the range ω_e for which the system (3.2) has a three-dimensional stable manifold (Regardless of the eigenvalue being zero), one applies Routh-Hurwitz stability criterion to $Q(\lambda)$. So, all its roots have negative real parts if and only if the following conditions are satisfied

$$\begin{cases} 5\,|w_e| - 23.4 > 0, \\ 24.5\,|w_e| - 135.25 > 0, \\ -22.5\,|w_e|^2 + 331.55\,|w_e| - 1038.3 > 0, \end{cases} \tag{3.8}$$

Hence,

$$5.5204 < |w_e| < 10.221,$$

In contrast, chaos has a greater possibility of occurrence if (3.7) has one or more roots with positive real parts, that is

$$|w_e| < 5.5204, \quad \text{or} \quad |w_e| > 10.221. \tag{3.9}$$

According to the above results, we deduce that the initial value of the state variable $\omega(t)$ can affect considerably the dynamical behavior of the system (3.2).

3.2 Bifurcation and Lyapunov Exponents spectrum

3.2.1 Dynamical behaviors versus the parameter a

In this section, the parameters take the following values $\alpha = 5, \beta = 5, \gamma = 0.1, b = 1, \xi = 3$ and let a vary over a certain interval to discuss the complex dynamics of the system (3.2) with the initial condition $(x, y, z, w_0) = (-0.5, 0.1, 0.01, -1)$. The bifurcation diagram of y and the corresponding Lyapunov exponents spectrum for a varying from 0 to 6 with a step size $h = 0.001$ are obtained as depicted in Figure 3.1 and Figure 3.2, respectively, which are

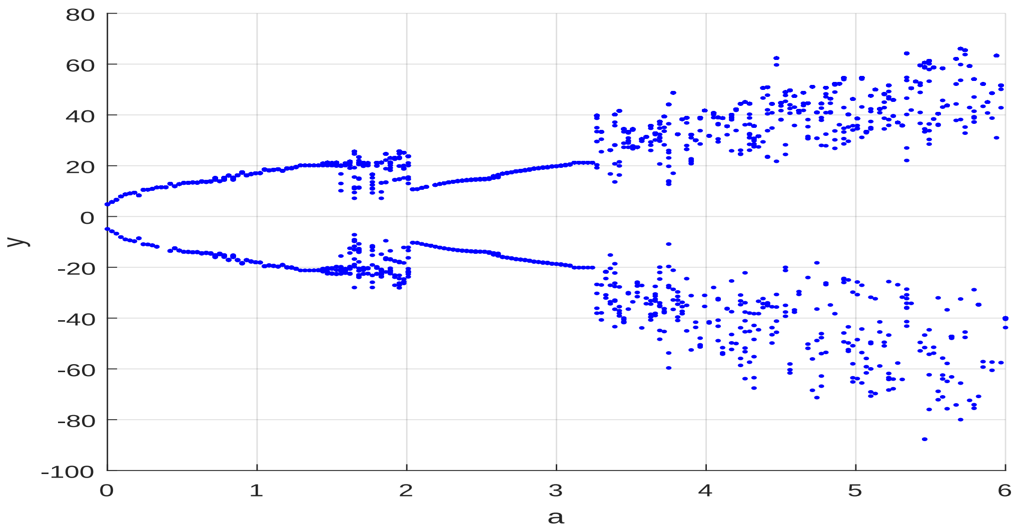

Figure 3.1: Bifurcation diagram with respect to the parameter a for $w_0 = -1$

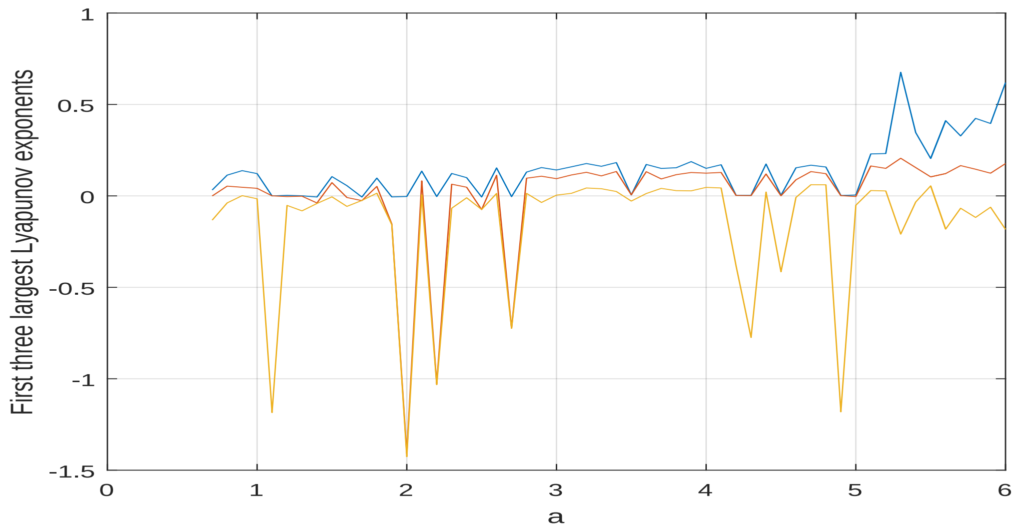

Figure 3.2: The three largest Lyapunov exponents of the system (3.2) versus the parameter a for $w_0 = -1$

in good coincidence.

From these figures it is obvious that system (3.2) displays period 1 orbit for $a \in]0.02, 1.41[\cup]2.04, 3.24[$. For $a \in]1.41, 2.1[\cup]3.24, 6[$ system (3.2) demonstrates chaotic and hyperchaotic behavior.

In particular, for $a = 3$ the Lyapunov exponents are

$$L_1 \approx 0.1417,\ L_2 \approx 0.0942,\ L_3 \approx 0.042,\ L_4 \approx -52.2119. \tag{3.10}$$

Since $L_1 + L_2 + L_3 + L_4 = -51.9719 < 0$, $L_1 > 0, L_2 > 0$, then the system (3.2) is hyperchaotic. The Kaplan-Yorke dimension of its attractor is

$$D_{KY} \approx 3 + \frac{L_1 + L_2 + L_3}{|L_4|} = 3 + \frac{0.1417 + 0.0942 + 0.042}{51.2119} = 3.0046, \tag{3.11}$$

which is a fractal dimension.

3.2.2 Dynamical behaviors versus the initial state w_0

In the aim to study the impact of initial condition values on the dynamical behavior of the system (3.2), for the set of parameter values (7), different diagrams are presented to identify chaos.

Considering the initial condition $(x, y, z, w_0) = (-0.5, 0.1, 0.01, w_0)$, the Lyapunov exponents spectrum and the corresponding bifurcation diagram of y, for w_0 varying from -15 to 15 with step 0.01 are obtained as shown in Figure 3.4 and Figure 3.5, respectively. From these diagrams, one observes that when the value of initial state w_0 belongs to the following four intervals: $[-15, -11.91]$, $[-5.52, -0.9]$, $[0.9, 5.52]$, $[11.91, 15]$, then system (3.2) exhibits chaos. Furthermore, the two diagrams indicate symmetry versus $w_0 = 0$.

Particularly, for $w_0 = -1$ the Lyapunov exponents are [7]

$$L_1 = 0.1485,\ L_2 = 0.0420,\ L_3 = -0.0154,\ L_4 = -31.7725. \tag{3.12}$$

Since $L_1 + L_2 + L_3 + L_4 = -31.5975 < 0$, $L_1 > 0, L_2 > 0$, then the system (3.2) is hyperchaotic. The Kaplan-Yorke dimension of its attractor is

$$D_{KY} = 3 + \frac{L_1 + L_2 + L_3}{|L_4|} = 3 + \frac{0.1485 + 0.0420 - 0.0154}{31.7725} = 3.0055, \tag{3.13}$$

which is a fractal dimension.

Some phase portraits are depicted in Figure 3.3 for different values of the initial condition w_0. In particular, a period-1 orbits are shown in 3.3(b), 3.3(e), and 3.3(h). Moreover, 3.3(c), 3.3(g) represents a stable equilibrium point, and 3.3(a), 3.3(d), 3.3(f) and 3.3(i) displays chaotic attractors.

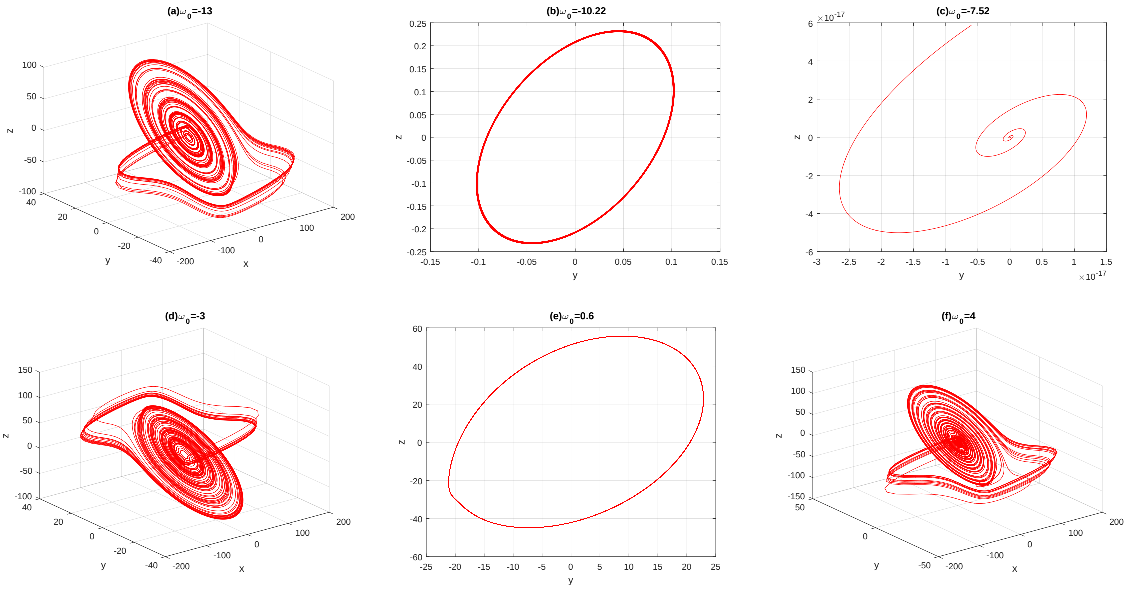

Figure 3.3: Some attractors for different values of initial condition w_0 : (a) $w_0 = -13$, (b) $w_0 = -10.22$, (c) $w_0 = -7.52$, (d) $w_0 = -3$, (e) $w_0 = 0.6$, (f) $w_0 = 4$, (g)

4 Modified projective synchronization between integer-order and incommensurate fractional order hyperchaotic systems

This section presents a theoretical analysis of the modified projective synchronization between integer-order and incommensurate fractional order hyperchaotic systems by applying the active control method based on the stability theorem of fractional-order linear systems.

4.1 Theoretical analysis

Giving two hyperchaotic systems: master and slave described respectively by :

$$\dot{X} = F(X), \tag{4.1}$$

$$D^{\alpha} Y = G(Y), \tag{4.2}$$

in order to make the study easier, (4.2) is rewritten as:

$$D^{\alpha} Y = AY + g(Y) + U, \tag{4.3}$$

where $X(t) = (x_1, x_2, ..., x_n)$, $Y(t) = (y_1, y_2, ..., y_n)$ are states of the master and the slave systems, respectively, $\alpha = (\alpha_1, \alpha_2, ..., \alpha_n)$ where $0 < \alpha_i < 1$ is the fractional-order, $A \in \mathbb{R}^{n \times n}$, g are the linear part and the nonlinear part of the system (4.3), respectively, and $U = (u_1, u_2, ..., u_n)$ is a control input vector.
The error state is defined as:

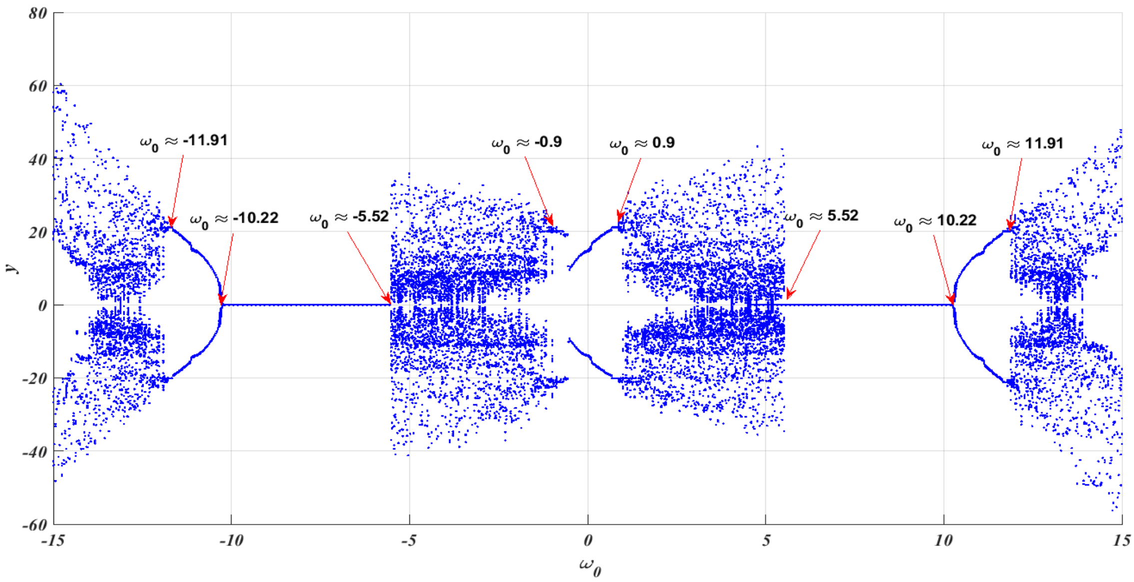

Figure 3.4: Bifurcation diagram with respect to the fourth coordinate w_0 of initial condition for $b = 1$

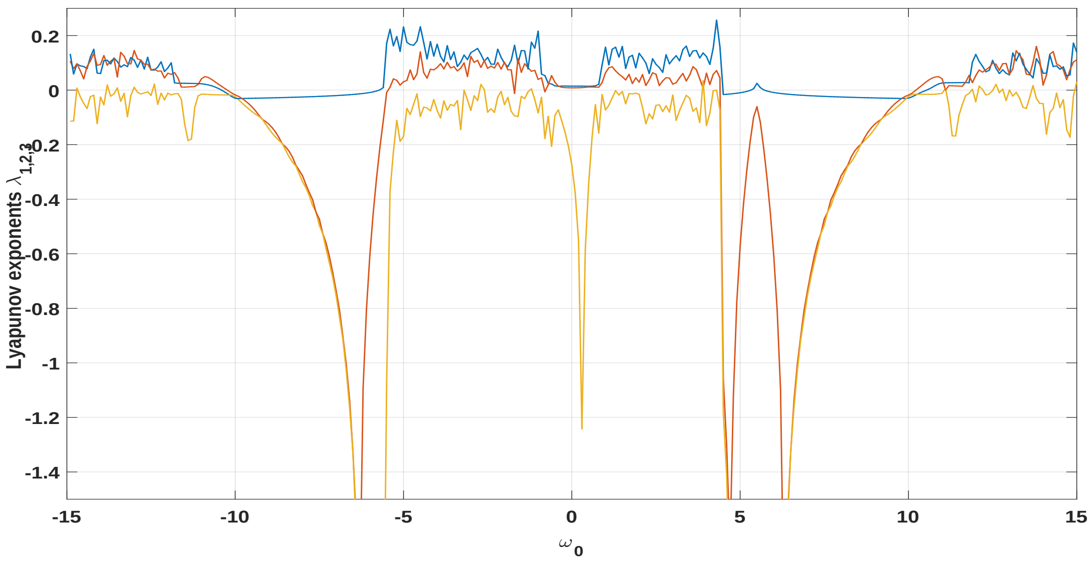

Figure 3.5: The three largest Lyapunov exponents of the system (3.2) versus the parameter w_0 for $b = 1$

$$e(t) = CY - X. \tag{4.4}$$

Where $C = diag(c_1, c_2, ..., c_n)$ denotes a scaling matrix. The objective of our work is to achieve synchronization between the two hyperchaotic systems (4.1) and (4.2) which could be achieved using the MPS technique when:

$$\lim_{t \to +\infty} e(t) = \lim_{t \to +\infty} \| CY(t) - X(t) \| = 0. \tag{4.5}$$

Hence the error system from equations (4.1) and (4.3) is as follows:

$$\begin{aligned} D^\alpha e &= CD^\alpha Y - D^\alpha X, & (4.6)\\ &= CAY + Cg(Y) + CU - D^\alpha X. & (4.7) \end{aligned}$$

In order to realize the MPS between integer order and incommensurate fractional order hyperchaotic systems, an active control U is chosen whereas the error system (4.4) asymptotically converges to zero. To achieve the stability of the system, we take the active control $U = (u_1, u_2, ..., u_n)^T$, such that:

$$U = C^{-1}((A + M)e - CAY - Cg(Y) + D^\alpha X), \tag{4.8}$$

where $M \in \mathbb{R}^{n \times n}$ is a gain matrix to be determined.
Substituting (4.8) into (4.7)yields :

$$D^\alpha e = (A + M)e. \tag{4.9}$$

Proposition 4.1. *If the matrix M is selected such that all roots λ_i of the characteristic equation:*

$$det(diag([\lambda^{m\alpha_1}, \lambda^{m\alpha_2}, ..., \lambda^{m\alpha_n}]) - (A + M)) = 0,$$

satisfy $|arg(\lambda_i)| > \frac{\pi}{2m}$, $i = 1, 2, ..., n$, where m is the least common multiple of the denominators of α_i, then the master system (4.1) and slave system (4.3) can be synchronized under the controller (4.8).

Proof. Immediately, using **theorem** 2.2. □

4.2 Numerical example and simulation results

To confirm the theoretical results obtained in the above sections, we perform numerical simulation by adopting the novel hyperchaotic system as a master system and its incommensurate fractional order version as a slave system.
The master system is defined as

$$\begin{cases} \dot{x}_1 = \alpha[x_3 + \xi x_1 - (-a + b|\omega|)x_1], \\ \dot{x}_2 = x_2 - x_3, \\ \dot{x}_3 = -\beta(x_1 - x_2) - \gamma x_3, \\ \dot{x}_4 = x_1, \end{cases} \tag{4.10}$$

The slave system is expressed by

$$\begin{cases} D^{\alpha_1} y_1 = \alpha[y_3 + \xi y_1 - (-a + b|\omega|) y_1] + u_1, \\ D^{\alpha_2} y_2 = y_2 - y_3 + u_2, \\ D^{\alpha_3} y_3 = -\beta(y_1 - y_2) - \gamma y_3 + u_3, \\ D^{\alpha_4} y_4 = y_1 + u_4, \end{cases} \tag{4.11}$$

where $u_1, u_2, ..., u_4$ are the active control functions, and α is a rational number between 0 and 1. The linear part of the system (4.3) is given by

$$A = \begin{bmatrix} \alpha(a+\xi) & 0 & \alpha & 0 \\ 0 & 1 & -1 & 0 \\ -\beta & \beta & -\gamma & 0 \\ 1 & 0 & 0 & 0 \end{bmatrix} \tag{4.12}$$

The matrix C is picked out in agreement with the MPS control technique proposed in equation (4.4) then

$$C = diag(5, 10, 0.1, 12), \tag{4.13}$$

and the gain matrix M is chosen as

$$M = \begin{bmatrix} -\alpha\xi - 2\alpha a & 0 & 1-\alpha & 0 \\ 0 & -2 & 1 & 0 \\ \beta & -\beta & -\gamma & 0 \\ -1 & 0 & 0 & -1 \end{bmatrix} \tag{4.14}$$

With the values given in (4.8) and (4.14), the error system becomes

$$\begin{bmatrix} D^{\alpha_1} e_1 \\ D^{\alpha_2} e_2 \\ D^{\alpha_3} e_3 \\ D^{\alpha_4} e_4 \end{bmatrix} = \begin{bmatrix} -\alpha a & 0 & 1 & 0 \\ 0 & -1 & 1 & 0.11 \\ 0 & 0 & -\gamma & 0 \\ -1.5 & 0 & 0 & -1 \end{bmatrix} \begin{bmatrix} e_1 \\ e_2 \\ e_3 \\ e_4 \end{bmatrix} \tag{4.15}$$

and the characteristic equation:

$$det(diag([\lambda^{m\alpha_1}, \lambda^{m\alpha_2}, \lambda^{m\alpha_3}, \lambda^{m\alpha_4}]) - (A + M)) = 0, \tag{4.16}$$

it can be transformed to:

$$(\lambda^{m\alpha_1} + 7.5)(\lambda^{m\alpha_2} + 1)(\lambda^{m\alpha_3} + 0.11)(\lambda^{m\alpha_4} + 1) = 0, \tag{4.17}$$

Where m is the least common multiple of the denominators of α_i, for $i = 1,2,3$ and 4, the master system (4.10) and the slave system (4.11) are synchronized if all roots λ of (4.17) satisfy $|arg(\lambda_i)| > \frac{\pi}{2m}$.

Let us take $(\alpha, \beta, \xi, a, \gamma) = (5, 5, 3, 1.5, 0.11)$ and $(\alpha_1, \alpha_2, \alpha_3, \alpha_4) = (0.95, 1, 1, 1)$, substituting in (4.17) yields:

$$(\lambda^{19} + 7.5)(\lambda^{20} + 1)(\lambda^{20} + 0.11)(\lambda^{20} + 1) = 0, \tag{4.18}$$

Obviously, all roots λ_i of (4.18) must satisfy the condition $|arg(\lambda_i)| > \frac{\pi}{40}$, consequently the master system (4.10) and the slave system (4.11) are synchronized, under the controller (4.8).

Finally, for numerical simulation, the Adams method [16] is used to solve the systems with time step size $h = 0.02$, the error system has the initial values:

$$e_1(0) = 0.1, e_2(0) = 0.2, e_3(0) = 0.1, e_4(0) = -1.$$

The parameter values of the hyperchaotic systems are taken as in the hyperchaotic case (**??**) and the different fractional-orders are taken as:

$$(\alpha_1,\ \alpha_2,\ \alpha_3,\ \alpha_4) = (0.95, 1, 1, 1).$$

Figure 4.1 illustrates the attractors of the novel incommensurate fractional order system (4.11).
Figure 4.2 illustrates the synchronization errors between integer-order and incommensurate fractional order systems.
Figure 4.3 illustrates the error functions evolution (4.15).
From Figure 4.3, for the given parameters, numerical results clearly show that errors converge to zero, and so the MPS is effectively implemented under the controller (4.8).

5 Conclusion

The synchronization between integer-order and fractional-order versions of a new memristor-based circuit with hyperchaotic dynamics was examined in this study. In order to derive the dynamical analysis, the stability theorems for fractional-order systems were applied, and the findings show that the variation of the fractional-order derivative significantly affects the proposed model's dynamical behavior. An MPS controller for synchronizing two hyperchaotic systems with integer and incommensurate fractional orders has been developed. Some numerical simulations have been provided to illustrate the theoretical results. We will use the proposed memristor-based hyperchaotic circuit for secure communication in the future by modulating the original signals into the chaotic sequences generated by the master circuit and transferring the combined signals to the receiver over a communication channel. Signals are received, and the MPS controller decodes them using the slave memristor-based circuit. Therefore, the relevant research is still in its early stages, and our next articles will discuss circuit implementations.

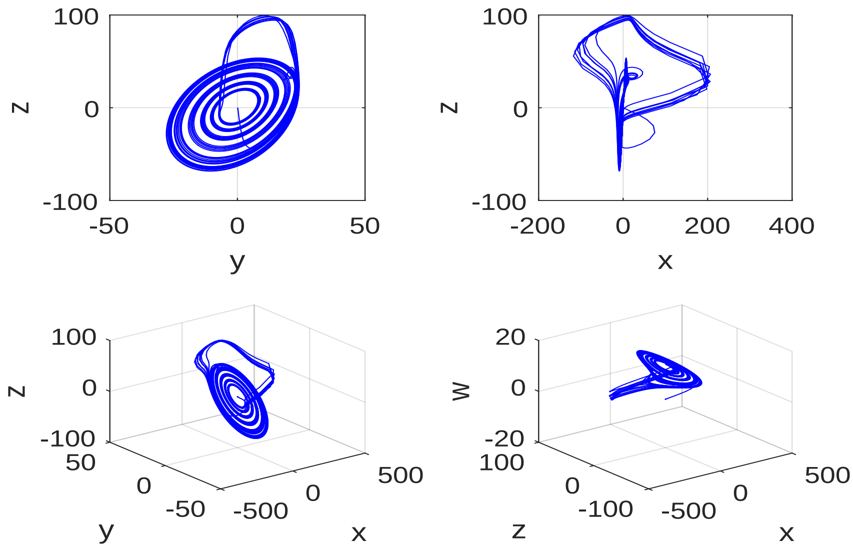

Figure 4.1: Some chaotic attractors of novel incommensurate fractional order system (4.11)

Declarations

Availability of data and materials

Data sharing not applicable to this article.

Funding

Not applicable.

Conflict of Interest

The authors have no conflicts of interest to declare.

References

[1] A. Boulkroune and M. Msaad, *On the design of observer-based fuzzy adaptive controller for nonlinear systems with unknown control gain sign*, Fuzzy Sets. Syst., **201** (2012), 71-85. DOI

[2] A. Boulkroune, S. Hamel, F. Zouari, and A. Leas, *Output-Feedback Controller Based Projective Lag Synchronization of Uncertain Chaotic Systems in the Presence of Input Nonlinearities*, Mathematical Problems in Engineering, **81** (2017), 1-12. DOI

[3] A. Chen, J. Lu, Jinhu Lü and S. Yu, *Generating hyperchaotic Lü attractor via state feedback control*, Physica A, **364** (2006), 103-110. DOI

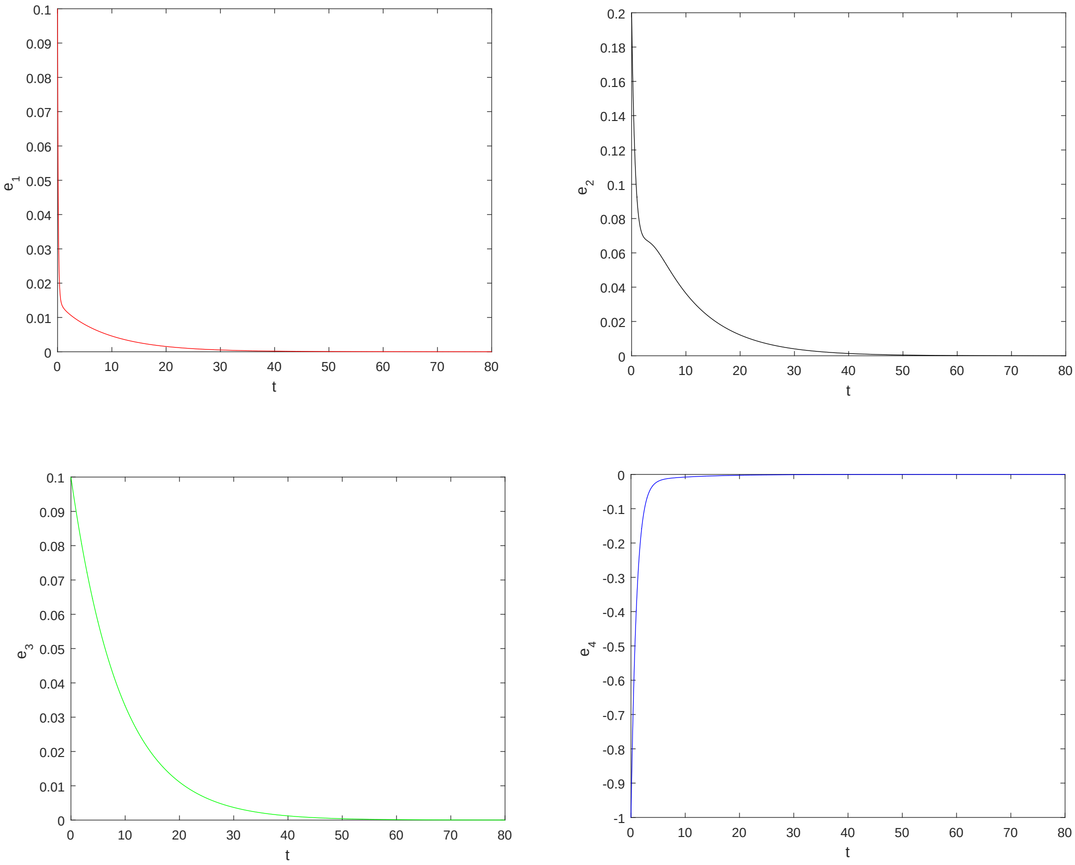

Figure 4.2: Synchronization errors between integer order and incommensurate fractional order systems

[4] M. M. Al-Sawalha, and A. Al-Sawalha, *Anti-synchronization of fractional-order chaotic and hyperchaotic systems with fully unknown parameters using modified adaptive control*, Open Phys., **14**(1) (2016), 304-313.

DOI

[5] A. Soukkou and S. Leulmi, *Controlling and Synchronizing of Fractional-Order Chaotic Systems via Simple and Optimal Fractional-Order Feedback Controller*, International Journal of Intelligent Systems Technologies and Applications., **8**(6) (2016), 56-69. DOI

[6] A. Soukkou, A. Boukabou and S. Leulmi, *Prediction-based feedback control and synchronization algorithm of fractional-order chaotic systems*, Nonlinear Dyn. **58**(4) (2016), 2183-2206. DOI

[7] A. Wolf, J. B. Swift, H. L. Swinney and J. A. Vastano, *Determning Lyapunov Exponents from a Time Series*, Physica D., **16** (1985), 285-317. DOI

[8] B. C. Bao, J. P. Xu and Z. Liu, *Initial state dependent dynamical behaviors in memristor based chaotic circuit*, Chinese Physics Letters, **27**(7) (2010), 070504. DOI

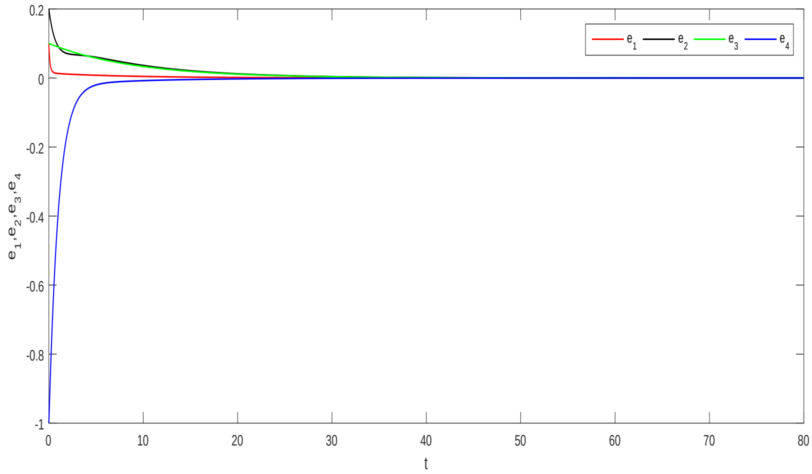

Figure 4.3: The synchronization errors of (4.10) and (4.11)

[9] B. Muthuswamy and P. P. Kokate, *Memristor based chaotic circuits*, IETE Technical Review. **26**(6) (2009), 415-426. DOI

[10] B. Wang, J. Jian and H. Yu, *Adaptive synchronization of fractional-order memristor-based Chuas system*, Systems Science, (2014), 291-296. DOI

[11] D. Cafagna and G. Grassi, *On the simplest fractional-order memristor-based chaotic system*, Nonlinear Dyn., **70**(2)(2012), 1185-1197. DOI

[12] G. Ye and J. Zhou, *A block chaotic image encryption scheme based on self-adaptive modelling*, Applied Soft Computing, **22**(2014), 351-357. DOI

[13] I. Petráš, *Fractional-order memristor-based Chua's circuit*, IEEE Trans. Circuits Syst. II., **57**(12) (2010), 975-979. DOI

[14] J. Borghetti, G. S. Snider , P. J. Kuekes, J. J. Yang, D. R. Stewart and R. S. Williams, *Memristive switches enable tateful logic operations via material implication*, **64**(4) (2010), 873-876. DOI

[15] J. Wang and Z. Chen, *A novel hyperchaotic system and its complex dynamics*, Int. J. Bifurcation Chaos, **18**(11) (2008), 3309-3324. DOI

[16] K. Diethelm, N. J. Ford and A. D. Freed, *Detailed error analysis for a fractional Adams method*, Numer. Algorithms., **36** (2004), 31-52. DOI

[17] K. Murali and M. Lakshmanan, *Secure communication using a compound signal from generalized chaotic systems*, Phys. Lett. A., **241**(6) (1998), 303-310. DOI

[18] L. Jian , L. Shutang and Y. Chunhua, *Modified generalized projective synchronization of fractional-order chaotic Lü systems*, Adv. Differ. Equations, (2013), 2013-374. DOI

[19] L. Kocarev and U. Parlitz, *General approach for chaotic synchronization with application to communication*, Phys. Rev. Lett., **74** (1995), 5028-5031. DOI

[20] L. O. Chua, *Memristor, the missing circuit element*, IEEE Trans. circuit. Theory., **18** (1971), 507-519. DOI

[21] L. Teng, H. C. Iu Herbert , X. Y. Wang and X. K. Wang, *Chaotic behavior in fractional-order memristor-based simplest chaotic circuit using fourth degree polynomial*, Nonlinear Dyn., **77**(1-2) (2014), 231-241. DOI

[22] M-S. Abdelouahab, N-E. Hamri and J. Wang, *Hopf bifurcation and chaos in fractional-order modified hybrid optical system*, Nonlinear Dyn., **69**(1) (2012), 275–284. DOI

[23] M-S. Abdelouahab and R. Lozi, *Hopf bifurcation and chaos in simplest fractional-order memristors-based electrical circuit*, Indian Journal of Industrial and Applied Mathematics, **6**(2)(2015), 105-119. DOI

[24] M-S. Abdelouahab, R. Lozi and L. O. Chua, *Memfractance: a mathematical paradigm for circuit elements with memory*, Int. J. Bifurcation Chaos., **24**(9) (2014), 1430023 (29 pages). DOI

[25] M. Bharathwaj, Khalil, *Implementing memristor based chaotic circuit*, Int. J. Bifurcation Chaos, **20**(5) (2010), 1335-1350. DOI

[26] M. Itoh and L. O. Chua, *Memristor Oscillators*, Int. J. Bifurcation Chaos, **18**(11) (2008), 3183-3206. DOI

[27] O. E. Rossler, *An equation for hyperchaos*, Phys. Lett. A., **71**(2-3) (1979), 155-177. DOI

[28] Q. Li, S. Hu, S. Tang and G. Zeng, *Hyperchaos and horseshoe in a $4-D$ memristive system with a line of equilibria and its implementation*, Int. J. Circuit Theory Appl., **42**(11) (2014), 1172-1188. DOI

[29] R. Suresh, and V. Sundarapandian, *Hybrid synchronization of n–scroll Chua and Lur'e chaotic systems via backstepping control with novel feedback*. Arch. Control Sci., **3** (2012), 343-365. DOI

[30] Sh. Wang, Xi. Wang and Y. Zhou, *A Memristor-Based Complex Lorenz System and Its Modified Projective Synchronization*, Entropy.,**17**(11) (2015), 7628-7644. DOI

[31] S. Kaouache and M-S. Abdelouahab, *Modified Projective Synchronization between Integer Order and fractional-order Hyperchaotic Systems*, Journal of Adv Research in Dynamical and Control Systems, **10**(5) (2018), 96-104.

[32] S. Rasappan, Y. Li , X. Huang, Y. Song and J. Lin, *A new fourth-order memristive chaotic system and its generation*, Int. J. Bifurcation Chaos, **25**(11) (2015), 1550151. DOI

[33] S. Shin, K. Kim and S. M. Kang , *Memristor applications for programmable analog ICs*, IEEE Transactions in Nanotechnology, **10**(2) (2011), 266-274. DOI

[34] S. Vaidyanathan, Ch. K. Volos and V.-T. Pham, *Analysis, Control, Synchronization and SPICE Implementation of a Novel 4-D Hyperchaotic Rikitake Dynamo System without Equilibrium*, Journal of Engineering Science and Technology Review, **8** (2)(2015), 232-244. DOI

[35] S. Vaidyanathan, Ch. K. Volos and V. -T. Pham, *Analysis, adaptive control and adaptive synchronization of a nine-term novel 3-D chaotic system with four quadratic nonlinearities and its circuit simulation*, Journal of Engineering Science and Technology Review, **8**(2) (2015), 174–184. DOI

[36] T. I. Chien and T. L. Liao, *Design of secure digital communication systems using chaotic modulation, cryptography and chaotic synchronization*, Chaos, Solitons Fractals, **24** (2005), 241-245. DOI

[37] V. T. Pham, Ch. Volos and L. V. Gambuzza, *A Memristive Hyperchaotic System without Equilibrium*, The Scientific World Journal, 368986 (2014), 1-9. DOI

[38] W. Zhen, H. Xia and S. Hao, *Control of an uncertain fractional-order economic system via adaptive sliding mode*, Neurocomputing, **83** (2012), 83-88. DOI

[39] X. Huang, J. Jia, Y. Li and Z. Wang, *Complex Nonlinear Dynamics in fractional and integer order memristor-based systems*, Neurocomputing., **218**(19) (2016), 296-306. DOI

[40] H. Xi, Y. Li, and X. Huang. *Generation and Nonlinear Dynamical Analyses of Fractional-Order Memristor-Based Lorenz Systems*, Entropy, **16**(12) (2014), 6240-6253. DOI

[41] X. J. Wu and Y. Lu, *Generalized projective synchronization of the fractional-order Chen hyperchaotic system*, Nonlinear Dyn., **57**(1-2) (2009), 25-35. DOI

[42] Y. V. Pershin and M. D. Ventra , *Experimental demonstration of associative memory with memristive neural networks*, Neural Networks, **23**(7) (2010), 881-886. DOI

[43] Y. Yu and H. Li, *The synchronization of fractional-order Rossler hyperchaotic systems*, Physica A, **387** (5-6)(2008), 1393-1403. DOI

[44] Z. Elhadj, *Dynamical Analysis of a $3-D$ Chaotic System with only Two Quadratic Nonlinearities*, J. Syst. Sci. Complex., **21**(1) (2008), 67-75. DOI

[45] Z. Hrubš and T. Gotthans, *Analysis and synthesis of chaotic circuits using memristor properies*, Journal of electrical engineering, **65**(3) (2014), 129-136. DOI